Appl. Environ. Microbiol. doi:10.1128/AEM.00961-15

Acromyrmex leaf-cutting ants have simple gut microbiota with nitrogen-fixing potential

Panagiotis Sapountzis[1*], Mariya Zhukova[1,2], Lars H. Hansen[3], Søren J. Sørensen[3], Morten Schiøtt[1*], Jacobus J. Boomsma[1*]

[1] Centre for Social Evolution, Department of Biology, University of Copenhagen, Universitetsparken 15, 2100 Copenhagen, Denmark

[2] Institute of Cytology and Genetics, Siberian Branch of the Russian Academy of Sciences, 630090, Novosibirsk, Russia

[3] Molecular Microbial Ecology Group, Department of Biology, University of Copenhagen, Universitetsparken 15, 2100 Copenhagen, Denmark

Address for correspondence: Panagiotis Sapountzis, Centre for Social Evolution, Department of Biology, Universitetsparken 15, University of Copenhagen, DK-2100 Copenhagen, Denmark.
Phone: +45 35330374; Fax: +45 35321250;
[*]Corresponding author emails: sapountzis@bio.ku.dk, mschiott@bio.ku.dk and jjboomsma@bio.ku.dk

Short title: Gut microbiota of *Acromyrmex* ants

Abstract

Ants and termites have independently evolved obligate fungus-farming mutualisms, but their gardening procedures are fundamentally different as the termites predigest their plant substrate whereas the ants deposit it directly on the fungus-garden. Fungus-growing termites retained diverse gut microbiota, but bacterial gut communities in fungus-growing leaf-cutting ants have not been investigated so it is unknown whether and how they are specialized on an exclusive fungal diet. Here we characterize the gut bacterial community of Panamanian *Acromyrmex* species, which are dominated by only four bacterial taxa: *Wolbachia,* Rhizobiales and two Entomoplasmatales. We show that the Entomoplasmatales can be both intracellular and extracellular across different gut tissues, *Wolbachia* are mainly but not exclusively intracellular, while the Rhizobiales species is strictly extracellular and confined to the gut lumen where it forms biofilms along the hindgut cuticle supported by an adhesive matrix of polysaccharides. Tetracycline diets eliminated the Entomoplasmatales symbionts but hardly affected *Wolbachia* and only moderately reduced the Rhizobiales suggesting that the latter are protected by the biofilm matrix. We show that the Rhizobiales symbiont produces bacterial NifH proteins that have been associated with the fixation of nitrogen, suggesting that these compartmentalized hindgut symbionts alleviate nutritional constraints emanating from an exclusive fungus garden diet reared on a substrate of leaves.

Key words: biofilm, Entomoplasmatales, NifH, Rhizobiales, *Wolbachia*

Introduction

Communities of gut bacteria play key roles in nutrient acquisition, vitamin supplementation, and disease-resistance. Their diversity often co-varies with host diet, both across lineages with different ecological niches and between conspecific populations in different habitats or geographic regions (1–3). Elucidating the significance of single bacterial taxa in omnivores such as humans is dauntingly complex (3, 4), but insects with specialized diets have regularly offered gut microbiota study systems that are dominated by a limited number of species (5–7). Several insect-microbial symbioses are evolutionarily ancient so that extensive functional complementarity between hosts and symbionts could evolve, as in aphids that rely on *Buchnera* for the production of essential amino acids (8, 9). Other such mutualisms have more recent origins, such as bedbugs that rely on *Wolbachia* for vitamin B production (10, 11) or wood eating beetles that carry nitrogen-fixing gut bacteria in order to subsist on protein-poor diets (12).

The eusocial insects offer abundant niche space for bacterial symbionts (5, 13–16) because many have peculiar diets and practice liquid food transfer (trophallaxis), which facilitates symbiont transmission within colonies. Higher termites replaced their ancestral protist gut communities by bacterial microbiota (17), while other early studies identified *Blochmannia* gut symbionts in carpenter ants (18, 19) and a community of gut-pouch symbionts in *Tetraponera* ants (20, 21). More recently, comparative studies have started to survey the total complexity of gut microbiota of ants to reveal overall nutritional adaptations associated with predatory and herbivorous feeding habits (6, 14, 19), and comparable studies in termites documented the importance of gut microbes for the conversion of dead plant material into nutrients that can be absorbed (22–24). A similar approach has been successful in honey bees and bumble bees, and revealed microbiota dominated by rather few bacterial species, consistent with bees having more predictable pollen and nectar diets

than ants and termites with generalist feeding ecologies (5, 25–28). The dominant gut bacteria of bees first appeared to be primarily adaptive in providing hosts with partial protection against gut parasites, but evidence for nutritional supplementation has increasingly been found (25–27, 29).

Recent studies of the gut microbiota of fungus-growing termites offered remarkable confirmation of the putative association between simple diets and simple gut microbiota, as it appeared that foragers consuming leaf-litter and wood have complex microbiota, whereas a mature queen had a gut microbial community of strikingly low diversity consistent with an exclusive fungal diet (23). Because leaf-cutting ants consume mostly if not exclusively fungus, we would thus expect to find simple microbiota reminiscent of the microbial diversity in the guts of bees who also have specialized diets (pollen and nectar). Because pollen are rather protein-rich (30) relative to leaves (31), we would also expect leaf-cutting ant microbiota to have a higher likelihood of providing nutritional supplementation. This hypothesis is reinforced by a study that identified *Klebsiella* and *Pantoea* nitrogen-fixing bacteria in the fungus gardens of *Atta* leafcutter ants, but without investigating their gut bacterial communities (32).

We tested these expectations in *Acromyrmex* leaf-cutting ants. Using 16S-454 and 16S-Miseq sequencing we determined the major bacterial OTUs (Operational Taxonomic Units, representing a cluster of bacterial 16S sequences of ≥ 97% similarity; typically interpreted as representing a bacterial species) associated with the digestive system of these ants. We then used a combination of fluorescence and electron microscopy to investigate the localization of the major bacterial OTUs across gut tissues, the lumen and the surrounding fat bodies to obtain inferences about their putative adaptive roles. We subsequently kept ants on sterile sugar solutions with and without the antibiotic tetracycline and monitored changes in prevalence of dominant gut bacteria. Finally, we focused on

92 an extracellular Rhizobiales species that was restricted to the hindgut lumen and discovered that
93 these bacteria are embedded in a biofilm-like matrix of polysaccharides and produce NifH proteins,
94 which are known to mediate the reduction of free nitrogen to the bio-available NH_3.
95

96 ## Material and Methods

97 ***Ant collection and maintenance, sterile diets, DNA extractions, 454 pyrosequencing and Illumina***
98 ***Miseq sequencing***

99 Ant colonies were collected in Gamboa, Republic of Panama. We used 11 *Acromyrmex* lab colonies
100 for 454 sequencing (eight *A. echinatior*, two *A. octospinosus* and one *A. volcanus*) and 13 partly
101 overlapping *Acromyrmex* colonies for Miseq sequencing: six new colonies (sampled both in the
102 field and after being transferred to the lab) and seven lab colonies, more than two years after
103 collection (six of them already sequenced with 454). This double procedure was chosen because we
104 were seeking to verify that bacterial gut communities could be reproduced across sequencing
105 platforms and to elucidate their susceptibility to changes in rearing conditions (field vs. 3 months in
106 the lab vs. >2 years in the lab). An overview of the sampling and experimental procedures is
107 provided in Table S1. DNA for both 454 and Miseq sequencing was extracted with the same
108 methods (see details below), and all lab colonies were maintained in rearing rooms at ca. 25˚C and
109 70 % RH under a 12 hour photoperiod.
110

111 The ant workers that were reared on artificial diets were collected from lab colony Ae150, and were
112 picked from the fungus gardens with forceps and placed in groups of 15 in sterile Petri dishes
113 (90x15mm), which had an inverted screwcap in the middle that served as liquid food vial. Control
114 experiments used Petri dishes with 15 workers across four basic feeding regimes, FG: fructose (5 %
115 w/v) + glucose (5 %w /v), FGY: fructose (5 % w/v) + glucose (5 % w/v) + yeast extract (2 % w/v),

S_1: sucrose (10 % w/v), SY: sucrose (10 % w/v) + yeast (2 % w/v), and the antibiotic treatments used a fully comparable set of feeding regimes (FGT, FGYT, ST_1, SYT) with 1mg/ml tetracycline added. The S and ST treatments were duplicated (S_2 and ST_2) with 20 and 60 ant workers respectively and all diet-components were dissolved in sterile distilled water and filter sterilized. For an overall idea of the experimental setup see Figure S1B-S1D. Petri dishes were monitored every second day for ant mortality.

To obtain an estimate of the gut bacterial diversity of the ants on different diets without killing them, we collected fecal droplets once a week from 5 of the 15 workers from each group (day 7, 14, 21 and 28) and stored them in -80˚C until DNA extraction. Towards the end of the experiment (day 28 and 35) we dissected 2-5 still alive ants from each group (2 ants for each of the initial treatments (FG, FGY, S_1, SY, FGT, FGYT, ST_1, SYT) and 5 ants from the duplicated treatments (S_2 and ST_2)), collected all gut tissues, and pooled them into single treatment and control samples per colony.

To obtain the DNA samples for the 454-pyrosequencing, ant workers were anaesthetized on ice, surface-sterilized by submerging them into absolute ethanol for 60 seconds and then rinsed with sterilized distilled water. The ants were dissected in sterile phosphate buffered saline (PBS) under a stereo microscope and stored at -80˚C until DNA extraction. Five workers from each colony were dissected and all gut tissues collected, pooled in one sample, and frozen. All DNA samples were extracted from these frozen samples using the Qiagen Blood and Tissue kit following the manufacturer's instructions and including an extra step where glass beads of 0.5mm were added and the lysate was vortexed for 30s. All samples were re-eluted in 150 µl AE elution buffer. Bacterial DNA amplification and 454 pyrosequencing were performed as described previously (33).

Extracted DNA for the Miseq sequencing was sent to the Microbial Systems Laboratory at the University of Michigan for library preparation and sequencing.

Analyses of 454 and Miseq data

The 454 data were analyzed using Mothur (v.1.33.3) (34) after nine rounds of filtering as described in the standard operating procedure (SOP) protocol with few modifications (35) (page accessed July 2014): 1) sequences with homopolymer stretches longer than 10 bases were removed, 2) the filtered sequences were aligned against the Silva 111 non-redundant database (36), and 3) sequences were assigned to taxonomic groups using the Bayesian classifier implemented in Mothur with a confidence threshold of 80% while using the same Silva database. In these filtering steps we also included the pre.cluster command, based on the algorithm developed by Huse et al (37), and we removed all reads assigned to Mitochondria, Chloroplasts, Archaea or Eukaryota. We did not exclude "unknown sequences" but did not find any either after the classification was completed. Operational Taxonomic units (OTUs) were obtained by generating a distance matrix with pairwise distance lengths smaller than 0.15. The data were then clustered and each OTU was classified with a 97% similarity cut-off using the same databases as before. All data were deposited in Genbank under the accession numbers presented in Table S2.

Rarefaction tables were constructed with Mothur using pseudoreplicate OTU datasets containing between 1 and 13927 sequences with 1000 iterations per pseudo-replicate and the curves were visualized in Microsoft Excel 2013. The final OTU table was rarefied at 5800 reads and used for all downstream analyses including the calculation of Euclidean distances that were used for PCoA analyses in R. The read counts of the four most abundant OTUs were transformed to percentages,

entered into JMP 10.0, and used to perform non-parametric Spearman tests for correlations that could suggest mutual exclusiveness or reinforcement

For the Miseq data analysis we also used Mothur (v.1.33.3) (34) and performed several rounds of filtering as described in the SOP protocol (38) (page accessed October 2014) with the only difference that sequences were assigned to taxonomic groups using the Bayesian classifier implemented in Mothur with a confidence threshold of 80%. The final OTU table was rarefied at 28000 reads and used for all downstream analyses including the calculation of Euclidean distances that were used for PCoA analysis in R. We used an ANOVA regression to correlate Miseq relative abundances with qPCR absolute gene copy numbers for a random selection of samples (see text below).

We retrieved OTU sequences from both data sets using python scripts and compared them to each other and to specific probes using the BLAST algorithm with an 1e-50 evalue cutoff and 50% identity (39). In order to design primers and probes from the retrieved OTUs, sequences were aligned using the Map to Reference algorithm incorporated in Geneious software v4.8.5 and v7.0.6 (40).

For the ant survival analyses we used Cox proportional hazards models (with censoring), carried out with the coxph function of the Survival package of R (version 3.1.1), following assessment of proportional hazards using cox.zph (41, 42). The cofactors included the substrate, the presence of yeast, or the presence of tetracycline. Data were plotted using the survival analysis function in JMP 10.0. Effects of the different components of the diets on the presence/absence of certain bacterial groups in the guts and the fecal droplets were compared using pairwise multivariate correlations

186 across all samples. We constructed 2x2 contingency tables examining each of the bacterial species
187 and diet components and evaluated their distribution frequencies using Pearson χ^2 tests in JMP 10.0.
188 To validate bacterial presence in fecal droplets, we collected samples from the ants in experimental
189 petri dishes at day 7, 14, 21, 26 and 28, and used a Cox proportional hazard model (with censoring)
190 to analyze the data under the assumption that the number of days of bacterial survival in guts as
191 sampled from fecal droplets was equal to the number of days of obtaining positive bacterial signals
192 by dissections during the four weeks of monitoring (Figure S1C). The diet groups that had positive
193 bacterial signals in the fecal droplets until the last day of monitoring were considered censored.
194
195 ***PCR reactions***
196 To identify *nifH* sequences, we used a previously described protocol (14) and sequences identified
197 in colony Ae150 [accession number: KP256164] to design *nifH* specific primers (C8_nifH_F/R,
198 Table S3). These were then used either directly or to perform the second step of a nested PCR in
199 combination with primers in the protocol described previously and targeting the same region (14,
200 32). PCR conditions were: denaturation for 3 min at 94°C, followed by 40 cycles of 30 sec at 94°C,
201 30 sec at 60°C, 30 sec at 72°C and a 7-min final extension at 72°C. All PCR products were gel
202 purified (QIAquick gel extraction kit, Qiagen or Montage Gel Extraction kit, Millipore) and sent to
203 Eurofins (Germany) for sequencing. Samples with failing sequencing reactions or chromatographs
204 with multiple peaks were re-amplified and cloned using the TOPO TA cloning kit (Invitrogen). At
205 least 20 bacterial colonies from each cloning were checked with PCR using the C8-nifH primers,
206 and ten positive PCR products from each cloning were sent to MWG for sequencing. *NifH*
207 sequences were deposited in Genbank under accession numbers: [KF613173, KP256159-
208 KP256169].
209

16S-specific primers were constructed in Geneious for *EntAcro1* (Entomoplasmatales), *RhiAcro1* (Rhizobiales) and *EntAcro2* (Entomoplasmatales) (see Table S3). The specificity of the primers was confirmed by PCR, cloning and Sanger sequencing of various PCR products from different colonies which showed that the primers amplify the expected sequences (data not shown). To detect *WolAcro1* (*Wolbachia*), we used the *wsp*-specific primers (43). PCR conditions were: denaturation for 3 min at 94°C, followed by 35 cycles of 30 sec at 94°C, 30 sec at annealing temperature (see Table S3), 30 sec at 72°C, and a 7-min final extension at 72°C.

Quantitative PCR (qPCR)

A number of *A.echinatior* colonies (four lab (>2 years) and two field) and *A.octospinosus* colonies (two lab (>2 years) and one field) were used to evaluate the accuracy of the relative abundances of the four major OTUs (*EntAcro1*, *EntAcro2*, *RhiAcro1* and *WolAcro1*) obtained by 454 and Miseq sequencing. We targeted three out of the four major OTUs discovered in our study for which we had 16S-specific primers: Entom_F/Entom_A_R for *EntAcro1*, Entom_F/Entom_B_R for *EntAcro2* and Phyllo_F/Phyllo_R for *RhiAcro1* (Table S3) in reactions with SYBR Premix Ex Taq (Takara Bio Inc., St Germain en Laye, France) on the Mx3000P system (Stratagene, Santa Clara, CA, USA). Reactions took place in a final volume of 20ul containing 10ul buffer, 8.3ul ddH2O, 0.4ul of each primer (10mM), 0.4ul ROX standard and 0.5ul template DNA. PCR conditions were: denaturation for 2 min at 94°C, followed by 40 cycles of 30 sec at 94°C, 30 sec at annealing temperature (see Table S3), 30 sec at 72°C, followed by dissociation curve analysis. All qPCR reactions were replicated and the Ct (cycle threshold) mean was used as measure of relative gene abundance. Each run included two negative controls of no added template. All data were normalized relative to the ant EF-1α gene as control (44). For each gene that we analyzed, the initial template concentration was calculated from a standard curve with PCR product in tenfold dilution series of known

Applied and Environmental Microbiology

concentration, as quantified by nanodrop. To evaluate whether the Miseq relative abundances correlated with the bacterial 16S gene copy numbers we used ANOVA regression analysis in JMP 10.0.

Fluorescent in situ hybridization

Five to ten ant workers from colonies Ae150 for *A. echinatior* and colony Ao492 for *A. octospinosus* were dissected in PBS and their guts were placed in 4% paraformaldehyde for at least 24 hours. For the permeabilization, deproteinization, and hybridization we followed a previously described protocol (45). For the hybridization step we used 0.75 µg/µl specific labeled probes (Table S3) targeting bacteria belonging to the class of Mollicutes (order of Entomoplasmatales), and the class of Alpha-Proteobacteria (orders of Rhizobiales and Rickettsiales (*Wolbachia*)). As negative controls we used reverse probes for Entomoplasmatales and Rhizobiales (Table S3), which gave faint diffuse signals in the fat bodies that probably originated from lipid droplets of significantly different size and intensity than the bacteria-specific signals (Figure S2). To check permeabilization of cell membranes, we used DAPI staining as positive control in each experiment, because it has high cell permeability and therefore we confirmed that our specific probes were able to cross cell membranes similar to DAPI. We thus considered a signal as being specific when it was absent from the negative controls and co-localized with the DAPI bacterial staining. The FISH images were inspected and photographed using a Zeiss LSM 710 confocal microscope equipped with ZEN 2009 software and a Leica TCS SP2 microscope.

Immunofluorescence staining

Dissected tissues (digestive tract, fat body) of large workers were fixed in cold methanol (20 min, -20°C) and then permeabilized in cold acetone (5 min, -20°C). Samples were subsequently rinsed

three times with PBS with 0.1 % Triton-X 100 at RT (PBST) and incubated for 5 minutes in PBST. This was followed by incubation of tissues for 1 hr with 6 µg/ml affinity purified anti-NifH antibody (Agrisera, AS01 021A) diluted in PBS-TBSA (PBS, 0.1 % v/v Triton-X-100, 1 mg/ml BSA). The specificity of the global NifH protein antibody has been checked with Western Blots by the manufacturer against a series of bacterial NifH proteins, and has among others predicted specificity for *Rhizobium meliloti* (Agrisera, AS01 021A). As negative controls, fixed and permeabilized tissues were incubated for 1hr with PBS-TBSA and without primary antibody (Figure S2). All samples were washed three times with PBST before being incubated in the dark with a goat anti-chicken IgY conjugated to Dylight 488 (Pierce, SA5-10070) for 45 min and being washed twice with PBS 0.1%v/v Triton-X-100. Finally, the tissues were mounted in Vectashield medium containing DAPI (Vector Laboratories, H-1500) and viewed under a SP5 Leica confocal microscope with 10X and 63X objectives.

Electron microscopy

Large workers of *A. echinatior* (Ae150) were dissected in 0.1 M phosphate buffer (pH 7.4) and ant digestive tracts were fixed in 2.5 % glutaraldehyde (Sigma) in 0.1 M sodium cacodylate buffer (pH 7.4) for 2.5 h. This was followed by washings in the same buffer and postfixation in 1 % OsO_4 for 1 h, after which samples were placed in 1 % aqueous solution of uranyl acetate for 12 h at 4 °C. Samples were then dehydrated in ethanol series and acetone, and embedded in Agar 100 Resin (Agar Scientific Ltd.) or Spurr low-viscosity resin (Ted Pella Inc.). Ultra-thin sections were stained with uranyl acetate and Reynolds lead citrate and examined with a transmission electron microscope (JEM 100 SX, JEOL or CM100, FEI).

Periodic Acid Schiff (PAS) staining

Digestive tracts from large workers of *A. octospinosus* (Ao492), either taken directly from their colony's fungus garden or after having spent two weeks on sterile sucrose diets, were fixed in 4 % paraformaldehyde in 0.1 M phosphate buffer (pH 7.4) overnight at +4^{o}C and subsequently dehydrated via a graded alcohol and histoclear (Sigma) series, followed by embedding in paraplast plus (Sigma). Sections were cut at 3-4 µm and dried on a hot plate at 36^{o}C. After dewaxing and rehydration, sections were treated with 1 % aqueous periodic acid for 10 min, washed for 5 min in running tap water, immersed in Schiff's reagent (Sigma) for 15 min and washed for 10 min in running tap water to develop the colour. Finally, sections were dehydrated in ethanol and histoclear and mounted in DPX to be viewed with a Leica DM 5000 B microscope.

Results

16S-454 and 16S-Miseq sequencing

Using a 97% sequence identity cut-off, we identified a total of 180 bacterial OTUs from the 454-pyrosequencing (Table S4A). Rarefaction curves were approaching saturation in all but one sample (Ao492), indicating that coverage was generally sufficient for community structure analyses. The four most abundant OTUs belonged to the Mollicutes (Entomoplasmatales: *EntAcro1, EntAcro2*) and Alphaproteobacteria (Rhizobiales: *RhiAcro1* and *Wolbachia*: *WolAcro1*) and jointly always accounted for > 97 % of the reads per sample (Figure 1A and Table S4A). Although the rarefaction curve for Ao492 did not plateau (Figure S3A), also this colony was included in the analyses because the four dominant OTUs were all present.

Ranked sample prevalences of OTUs 5-14 never exceeded 0.71%, while none of the other OTUs exceeded 0.07% per sample (Table S4A). *RhiAcro1* and *WolAcro1* were present in all eleven samples, and all samples had at least one of the Entomoplasmatales species, as *EntAcro1* was found

in nine samples, *EntAcro2* in six samples, and five samples had both. OTU 5 was also an Entomoplasmatales (*EntAcro3*; found in 9 samples), but OTU 6 (*ActAcro1*) was an Actinomycetales (*Pseudonocardia*) that was 99% identical to one of the two vertically transmitted cuticular actinomycete symbionts (Ps1) of *A. echinatior* and *A. octospinosus* (33, 46, 47). This OTU was found in the single gut sample of *A. volcanus* and in one of the two *A. octospinosus* gut samples, but not in the eight *A. echinatior* samples. None of the other OTUs was restricted to or specific for any of the three *Acromyrmex* ant-species (Table S4A). We further characterized the *RhiAcro1*, *EntAcro1* and *EntAcro2* OTUs using Sanger sequencing and obtained 982bp, 1282bp and 1340bp sequences, respectively, while the *WolAcro1* OTU has been characterized previously (48, 49). Maximum Likelihood phylogenetic trees showed that *RhiAcro1* is closely related to Rhizobiales strains identified in *Trachymyrmex urichii* of the attine lineage (Figure S4A), while *EntAcro1* appeared to be closely related to *Mesoplasma lactucae* and *EntAcro2* to *Entomoplasma freundtii* (Figure S4B).

To validate whether the overall rank order of dominant gut OTUs was independent of lab or field conditions during sampling, we sequenced a comparable set of dissected guts from field and lab colonies on a Miseq platform. Rarefaction curves were approaching saturation for all samples (Figure S3B), indicating that coverage was sufficient for community structure analyses. *Wolbachia* was similarly dominant in *A. echinatior* and *A. octospinosus* gut samples from the field, whereas *EntAcro1* and *RhiAcro1* were abundant in field guts of *A. octospinosus* but rare in field guts of *A. echinatior* (*EntAcro1* abundant in one but <1% in two other field colonies and *RhiAcro1* <1% in all three field colonies). Once again the *EntAcro1*, *EntAcro2*, *WolAcro1* and *RhiAcro1* accounted jointly for > 97 % of the reads per sample (Figure 1 and Table S4B), but this time there were two

exceptions, Ao708(F) and Ao710(3m), that had an additional Entomoplasmatales OTU (*EntAcro10*), in respective abundances of 31% and 24%.

The gut microbiota of these *A. echinatior* field colonies were often excessively dominated by *Wolbachia* (45.7%, 98.1% and 99.6%; Figure 1) and showed consistent directional change towards Rhizobiales three months after colonies were moved to the lab to become similar to the gut microbiota of *A. octospinosus* (Figure S5).

Principal Coordinates Analysis (PCoA) based on weighted Euclidean distances obtained from both the 454 and Miseq runs confirmed that the microbiota differed in a quantitative rather than qualitative manner across sampling categories (Figure 1 and Figure S5). The relative abundances of *EntAcro1* and *EntAcro2* were significantly negatively correlated (Spearman $\rho = -0.858$, $P < 0.0007$*), whereas a number of other prevalences also showed signs of positive or negative correlation (Figure S6) but without reaching significance. PCoA comparison of the four focal OTUs in the six samples that were sequenced on both platforms further showed that OTUs were highly reproducible in four cases and satisfactory reproducible in the two other cases (Figure S5). To validate our relative abundance estimates, we performed qPCR using 16S-specific primers on a subset of the samples sequenced with Miseq which showed that relative abundances obtained from the Miseq samples satisfactory predicted the bacterial 16S gene copy numbers for *EntAcro1*, *EntAcro2* and *RhiAcro1* (Figure S7).

Localization, morphology and robustness of Mollicutes and Alpha-Proteobacteria against tetracycline

We designed probes specific for Mollicutes and Alpha-Proteobacteria OTUs (see Table S3 for probe specificity details) and used Fluorescent *In Situ* Hybridization (FISH) and confocal microscopy to examine different gut tissues of worker ants from colonies Ae150 and Ao492 (Figure 2A). This showed that Entomoplasmatales were present in the fat body cells (Figure 2B) and all gut tissues (Figure 2C,2E,2F) of *A. echinatior* and *A. octospinosus*: the Malpighian tubules (Figure 2C), the ileum (Figure 2E), and the rectum (Figure 2F). However, *RhiAcro1* appeared to be restricted to the hindgut (ileum and rectum; Figure 2G, 2H), while *WolAcro1* was sparsely present in the hindgut (Figure 2G) and more abundantly in the fat body cells (Figure 2D), the latter confirming results of a previous *A. octospinosus* study (44).

We further investigated the morphology and localization of these bacteria using Transmission Electron Microscopy (TEM) in *A. echinatior*. This showed that the Entomoplasmatales had a coccoid shape, an approximate diameter of 0.7 µm, and no bacterial cell wall (Figure 2I,J), and that rod-shaped Rhizobiales could be recognized by dense cytoplasm, an average diameter of 0.4 µm, and a length range of 0.8-2.7 µm (Figure 2K). *Wolbachia* were also distinct because of their typical three-layered envelope and heterogeneous cytoplasm (Figure 2L). TEM analysis confirmed the distribution patterns that we found by FISH microscopy (Figure 2 B-H), and refined the resolution of the cellular localization of the bacteria. Mollicutes could thus be seen to occur across almost all gut tissues, both intracellularly (Figure 2I) and extracellularly in the gut where dividing cells could sometimes be observed (Figure 2J), while Rhizobiales occurred only extracellularly in the hindgut lumen (Figure 2G,H), and *Wolbachia* mostly intracellular in the fat body cells (Figure 2D) as also shown previously (44).

376 To assess the robustness of bacterial symbionts in and around the guts (in fat body cells and gut
377 tissues), ants were deprived of their fungus gardens and fed on different artificial sugar diets, which
378 showed that *WolAcro1* prevalence was not, and *RhiAcro1* prevalence only moderately, affected by
379 tetracycline, whereas *EntAcro1* and *EntAcro2* disappeared from all gut and fat body tissues when
380 ants spent 28 days on such diets (Figure S1). We also examined the presence of bacteria in the ant
381 fecal droplets with PCR, as the antibiotics treatment should make them disappear when free-living
382 in the gut lumen. This showed that the two Entomoplasmatales, which are normally found in
383 *Acromyrmex* fecal droplets, could no longer be retrieved after ants had been kept on tetracycline for
384 14 days, while *RhiAcro1* prevalence in fecal droplets decreased much more slowly, a decline that
385 was mostly due to the non-fungal diet with only a minor additional effect of tetracycline (Figure
386 S1). Similar decline patterns were found in the guts, with tetracycline accelerating the
387 disappearance of the Entomoplasmatales species, but only slightly affecting *RhiAcro1* until more
388 than a month had passed. *Wolbachia* has previously been reported, albeit in highly variable cell
389 numbers, from fecal droplets of both *A. echinatior* and *A. octospinosus* (44, 50), and was only
390 sporadically found in the feces of the ants that we took directly from fungus gardens or exposed to
391 prolonged artificial sugar diets. Such diets completely eliminated *Wolbachia* from the fecal
392 droplets, but never from the gut tissues, suggesting that a fungal diet may be essential for
393 maintaining these bacteria in the gut lumen (Figure S1).
394
395 ***NifH protein production and co-localization with Rhizobiales in the hindgut***
396 Using degenerate primers, we identified multiple sequences of the *nifH* bacterial gene for
397 nitrogenase reductase, with colony Ae342 having three such sequences (pairwise identities 89.9%),
398 nine other colony samples having one *nifH* sequence, and colony Ae505 having zero. A Maximum
399 Likelihood tree using these and closely related sequences showed that 10/12 sequences are closely

Applied and Environmental Microbiology

400 related to *nifH* sequences originating from other Rhizobiales bacteria and 2/12 sequences
401 (18cl8_Ae342 and QC8_Ae342) are equally related to *nifH* sequences originating from both
402 Rhizobiales and non-Rhizobiales bacteria (Figure S8). Using micro-dissections and *nifH*-specific
403 PCR we found in two separate experiments that *nifH* sequence signals were abundant in the
404 hindgut, but weak and irregular in the Malpighian tubules and fat body cells (Figure 3A), and that
405 keeping workers on sterile sucrose solution without fungus-garden food for up to 15 days only
406 maintained *nifH* genes in the hindguts (Figure 3A).
407
408 To investigate whether some *nifH* sequences are transcribed into active NifH proteins we performed
409 Immunofluorescence (IF) confocal microscopy with a specific α-NifH antibody. This showed that
410 NifH proteins were present only towards the cuticular boundaries of the ileum and rectum, where
411 DAPI staining revealed that these NifH protein signals were localized in or immediately next to
412 bacterial DAPI signals (Figure 3B). TEM confirmed that only Rhizobiales bacteria were localized
413 close to the cuticle of the hindgut lumen (Figure 3C) and that these bacteria are surrounded by a
414 matrix that might facilitate both biofilm formation and attachment to the cuticle of the rectum and
415 ileum (Figure 3D,E). Rhizobiales were most abundant in the ileum (Figure 3E) and PAS staining of
416 hindgut sections showed consistent red staining corresponding to abundant polysaccharides in the
417 matrix where the Rhizobiales bacteria occurred (Figure 3F,G).
418

419 ## Discussion

420 ***Simple gut microbiota, uniform diets and intriguing actinomycetes***

421 Our results matched the expectation that gut microbiota of fungus-ingesting *Acromyrmex* leaf-
422 cutting ants should be dominated by relatively few OTUs. A bacterial gut community dominated by
423 few OTUs (what we refer to as "simple" here) has also been found in other eusocial insects with

424 relatively uniform diets, such as honey bees and bumble bees feeding on pollen and nectar (5, 28,
425 51) and cephalotine ants, which are mostly honeydew collecting functional herbivores (6). Our
426 results add yet another functionally herbivorous ant genus to the known Rhizobiales hosts (6, 14),
427 but also provide novel specifications about the location and function of these gut bacteria. In
428 particular, no other study has combined FISH and TEM and a-NifH IF to localize these major
429 endosymbionts of herbivorous ants (6, 14), showing that they are compartmentalized, aided by what
430 appears to be biofilm formation, and co-localized with bacterial NifH proteins, whose expression is
431 usually tightly regulated by oxygen and nitrogen levels (52).
432
433 When comparing prevalences of dominant gut bacteria in field and lab samples from the same
434 Panamanian field site, we generally found a good correspondence (Figure S5), except that *RhiAcro1*
435 and *EntAcro1* were sparse in the three *A. echinatior* field colonies (Figure S5 and Table S4B). This
436 may be related to the habitats of *A. echinatior* (open partly sun-lit areas) and *A. octospinosus*
437 (forest) being clearly distinct, and *A. echinatior* having somewhat higher fungal proteinase activity
438 in their field fungus gardens than *A. octospinosus* (53). The natural forage of *A. echinatior* colonies
439 may thus be less nitrogen-poor than the leaf fragments cut by *A. octospinosus* workers, but lab
440 colonies of both species received the same bramble-leaves (*Rubus* spec), a type of forage that likely
441 resembles natural *A. octospinosus* forage more than natural *A. echinatior* forage. *Wolbachia*
442 prevalences are known to differ between lab and field colonies of Panamanian *A. octospinosus*, as
443 they significantly increase in prevalence when colonies are moved indoors possibly due to relaxed
444 resource constraints (44).
445
446 Our results on fungus-growing leaf-cutting ants complement recent gut microbiota studies in
447 fungus-growing termites. These Macrotermitinae independently evolved farming of another

basidiomycete lineage, *Termitomyces*, but retained the termite habit of predigesting wood fragments and leaf-litter during a first gut passage before depositing primary feces as the substrate in which their fungal symbiont grows (54, 55). This broad diet of foraging workers and soldiers explains their complex gut microbiota (23, 56), but a resident *Macrotermes* queen was shown to have a simple gut community dominated by a single genus (*Bacillus*: > 98% joint prevalence), consistent with consuming only fungal food provided by the nursing workers (23). It thus appears that substrate ingestion rather than substrate handling may be decisive for the variability of bacterial gut communities of fungus-farming eusocial insects.

Low prevalences of cuticular *Pseudonocardia* bacteria were found in the worker guts of *A. volcanus* and *A. octospinosus* (*ActAcro1*: 0.71% of the reads in Av520 and 0.38% of the reads in AoDani). Panamanian *Acromyrmex* species differ in their typical abundance of cuticular *Pseudonocardia* (Ps) actinomycetes, with *A. volcanus* workers having very high coverage on their body (also in foragers), *A. octospinosus* workers having intermediate coverage, and *A. echinatior* workers having the lowest coverage ((57), personal observations), similar to our detection frequencies of these bacteria in the guts (Table S4). Further work will be needed to investigate whether the occasional presence of *ActAcro1* (99% similar to Ps1; 97% similar to Ps2 (33)) in the guts of *Acromyrmex* species has adaptive significance or is merely due to cuticular bacteria being ingested during allogrooming.

Spatial distributions of bacterial species within the* Acromyrmex *gut

RhiAcro1 was restricted to the hindgut, while *WolAcro1* and the Entomoplasmatales species were not (Figure 2; see also (44)). The latter two usually occur intracelullarly, which apparently necessitates an extra plasma membrane of ant origin to live in the host cytoplasm (Figure 2I,J,L).

Applied and Environmental Microbiology

Such extra plasma membranes have also been found in close relatives of Entomoplasmatales living in human reproductive organs (58) and have been hypothesized to protect bacteria against host immune defenses, a function that may also be relevant in *Wolbachia* (59, 60). The significant tendency towards mutual exclusion between *EntAcro1* and *EntAcro2* suggests that similar symbionts may compete for the same niche space in the host, and that complex additional interactions between the four dominant gut bacteria may exist as *WolAcro1* had a negative effect on *EntAcro1* and *RhiAcro1*, but a positive effect on *EntAcro2*. However these correlations should be tested in larger-scale and more in-depth studies to confirm mutual exclusiveness or reinforcement.

To our knowledge, the localization of insect-associated Rhizobiales has only been investigated in two previous studies and only at the overall organ level: one on *Tetraponera* ants (21) and one on *Odontotaenius* beetles (12). Our TEM and PAS analyses show that *Acromyrmex* Rhizobiales have the characteristic rod-shaped morphology of this genus (61) and are embedded in hindgut biofilms with a polysaccharide matrix as it has been demonstrated that the PAS-reagent stains specifically polysaccharides (62). This may help these *RhiAcro1* cultures to adhere to the hindgut lining and to maintain robustness when tetracycline reduces or terminates cell divisions. The ability of proteobacteria to synthesize extracellular polysaccharides for biofilm production has previously been demonstrated in host tissues of other insects (63) and on abiotic surfaces, usually mediated by a polar adhesive that is commonly found in Alpha-Proteobacteria (64).

***Putative functions of Rhizobiales, Entomoplasmatales and Wolbachia in* Acromyrmex**

RhiAcro1 and *WolAcro1* appear to be obligatorily associated with Panamanian *Acromyrmex* as symbionts because they were present in all samples investigated (Figure 1, Table S4) and were impossible to remove when feeding ants sugar solutions with tetracycline (Figure S1). This is

consistent with earlier studies showing that *Wolbachia* can survive for a month or more without proliferating (65) since a bacteriostatic antibiotic drug like tetracycline inhibits the growth but does not destroy the bacterial cells. Close relatives of *RhiAcro1* have been found in several other, mostly functionally herbivorous, ant species (6, 14, 66, 67), but Mollicutes (Entomoplasmatales) like *EntAcro1* (*Mesoplasma*) and *EntAcro2* (*Entomoplasma*) have mostly been found associated with predatory ants such as *Formica*, generalists such as *Polyrhachis*, and especially army ants have high prevalences most notably in the subfamily *Aenictinae* which are specialized predators of other ants and termites (68–70). In general, Entomoplasmatales are mostly intracellular pathogens and are not known to be part of biofilms, and a fairly close *Mycoplasma* relative is known to be sensitive to tetracycline (71) consistent with the rapid demise of *EntAcro1* and *EntAcro2* in our feeding experiments.

The possible function of the two Entomoplasmatales species remains enigmatic. Finding these bacteria intracellularly and in high cumulative abundances (Table S4) in healthy ant colonies would appear to be incompatible with these bacteria having a direct pathological impact on their host fitness. This interpretation is consistent with no bacterial symbionts of ants having been shown so far to be virulent in the pathogenic sense and multiple mutualistic functions having been suggested (6, 14, 70). The prevalence of Entomoplasmatales in several predatory ants (including army ants) and fungus-growing ants (they are also dominant in other higher attine ant species in Panama; Sapountzis et al, unpublished data) suggests that their function might be somehow related to the processing of chitin – the main component of the cuticles of insect-prey and fungal cell walls ingested by leaf-cutting ants – in spite of the insects producing their own chitinases. This, and the fact that Entomoplasmatales species associated with *Acromyrmex* ants vary in their potential mutual

519 exclusiveness and correlations with *Wolbachia* abundance offer interesting questions for further
520 research.
521
522 Rhizobiales closely related to *RhiAcro1* and other potentially nitrogen fixing endosymbionts have
523 been identified in several ants with protein-poor diets (6, 14, 20, 21, 32), while *Blochmania*
524 complements the diet of *Camponotus* ants (19, 72), suggesting these bacteria alleviate nitrogen
525 limitation and enhance colony growth. The combination of FISH, TEM and α-NifH
526 immunostaining, allowed us to show that NifH proteins are indeed produced in the very same
527 hindgut compartments where Rhizobiales were found, providing indications that these bacteria may
528 actively contribute nitrogen to the symbiosis. Tissue localization data in our present study and a
529 previous one (44) show that *Wolbachia* is abundantly present in various non-reproductive tissues
530 and in a free-living state in the crop (foregut) of *A. octospinosus*, suggesting that it may be a
531 mutualist with as yet unknown function (44) also because no clear reproductive manipulations by
532 *Wolbachia* infections (male killing, feminization, cytoplasmatic incompatibility) have so far been
533 demonstrated in ants (73, 74). All four OTU's that cumulatively make up more than 97% of the
534 *Acromyrmex* gut microbiota may thus be mutualists, but much further work will be needed to
535 specify the metabolic networks of these bacteria and to evaluate their benefits to the fungus-farming
536 symbiosis.
537

538 # References

539 1. **Engel P, Moran NA**. 2013. The gut microbiota of insects - diversity in structure and function. FEMS
540 Microbiol Rev **37**:699–735.

541 2. **Lee W-J, Hase K**. 2014. Gut microbiota-generated metabolites in animal health and disease. Nat Chem
542 Biol **10**:416–424.

543 3. **Lozupone CA, Stombaugh JI, Gordon JI, Jansson JK, Knight R**. 2012. Diversity, stability and resilience
544 of the human gut microbiota. Nature **489**:220–230.

4. **Tremaroli V, Bäckhed F**. 2012. Functional interactions between the gut microbiota and host metabolism. Nature **489**:242–249.

5. **Koch H, Schmid-Hempel P**. 2011. Bacterial communities in central european bumblebees: low diversity and high specificity. Microb Ecol **62**:121–133.

6. **Anderson KE, Russell JA, Moreau CS, Kautz S, Sullam KE, Hu Y, Basinger U, Mott BM, Buck N, Wheeler DE**. 2012. Highly similar microbial communities are shared among related and trophically similar ant species. Mol Ecol **21**:2282–2296.

7. **Douglas AE**. 2006. Phloem-sap feeding by animals: problems and solutions. J Exp Bot **57**:747–754.

8. **Shigenobu S, Watanabe H, Hattori M, Sakaki Y, Ishikawa H**. 2000. Genome sequence of the endocellular bacterial symbiont of aphids *Buchnera sp. APS.* Nature **407**:81–6.

9. **Baumann P, Baumann L, Lai C-Y, Rouhbakhsh D, Moran NA, Clark MA**. 1995. Genetics, physiology, and evolutionary relationships of the genus *Buchnera*: intracellular symbionts of aphids. Annu Rev Microbiol **49**:55–94.

10. **Hosokawa T, Koga R, Kikuchi Y, Meng XY, Fukatsu T**. 2010. *Wolbachia* as a bacteriocyte-associated nutritional mutualist. Proc Natl Acad Sci U S A **107**:769–774.

11. **Nikoh N, Hosokawa T, Moriyama M, Oshima K, Hattori M, Fukatsu T**. 2014. Evolutionary origin of insect-*Wolbachia* nutritional mutualism. Proc Natl Acad Sci U S A **111**:10257–10262.

12. **Ceja-Navarro JA, Nguyen NH, Karaoz U, Gross SR, Herman DJ, Andersen GL, Bruns TD, Pett-Ridge J, Blackwell M, Brodie EL**. 2014. Compartmentalized microbial composition, oxygen gradients and nitrogen fixation in the gut of *Odontotaenius disjunctus*. ISME J **8**:6–18.

13. **Sauer C, Stackebrandt E, Gadau J, Hölldobler B, Gross R**. 2000. Systematic relationships and cospeciation of bacterial endosymbionts and their carpenter ant host species: proposal of the new taxon *Candidatus Blochmannia gen. nov.* Int J Syst Evol Microbiol **50 Pt 5**:1877–1886.

14. **Russell JA, Moreau CS, Goldman-Huertas B, Fujiwara M, Lohman DJ, Pierce NE**. 2009. Bacterial gut symbionts are tightly linked with the evolution of herbivory in ants. Proc Natl Acad Sci U S A **106**:21236–21241.

15. **Hongoh Y**. 2010. Diversity and genomes of uncultured microbial symbionts in the termite gut. Biosci Biotechnol Biochem **74**:1145–1151.

16. **Warnecke F, Luginbühl P, Ivanova N, Ghassemian M, Richardson TH, Stege JT, Cayouette M, McHardy AC, Djordjevic G, Aboushadi N, Sorek R, Tringe SG, Podar M, Martin HG, Kunin V, Dalevi D, Madejska J, Kirton E, Platt D, Szeto E, Salamov A, Barry K, Mikhailova N, Kyrpides NC, Matson EG, Ottesen EA, Zhang X, Hernández M, Murillo C, Acosta LG, Rigoutsos I, Tamayo G, Green BD, Chang C, Rubin EM, Mathur EJ, Robertson DE, Hugenholtz P, Leadbetter JR**. 2007. Metagenomic and functional analysis of hindgut microbiota of a wood-feeding higher termite. Nature **450**:560–565.

17. **Breznak JA, Brune A**. 1994. Role of microorganisms in the digestion of lignocellulose by termites. Annu Rev Entomol **39**:453–487.

18. **Sauer C, Dudaczek D, Hölldobler B, Gross R**. 2002. Tissue localization of the endosymbiotic bacterium "*Candidatus Blochmannia floridanus*" in adults and larvae of the carpenter ant *Camponotus floridanus*. Appl Environ Microbiol **68**:4187–4193.

19. **Feldhaar H, Straka J, Krischke M, Berthold K, Stoll S, Mueller MJ, Gross R**. 2007. Nutritional upgrading for omnivorous carpenter ants by the endosymbiont *Blochmannia*. BMC Biol **5**:48.

20. **Stoll S, Gadau J, Gross R, Feldhaar H**. 2007. Bacterial microbiota associated with ants of the genus *Tetraponera*. Biol J Linn Soc **90**:399–412.

21. **Van Borm S, Buschinger A, Boomsma JJ, Billen J**. 2002. *Tetraponera* ants have gut symbionts related to nitrogen-fixing root-nodule bacteria. Proc Biol Sci **269**:2023–2027.

22. **Hongoh Y**. 2011. Toward the functional analysis of uncultivable, symbiotic microorganisms in the termite gut. Cell Mol Life Sci **68**:1311–1325.

23. **Poulsen M, Hu H, Li C, Chen Z, Xu L, Otani S, Nygaard S, Nobre T, Klaubauf S, Schindler PM, Hauser F, Pan H, Yang Z, Sonnenberg ASM, de Beer ZW, Zhang Y, Wingfield MJ, Grimmelikhuijzen CJP, de Vries RP, Korb J, Aanen DK, Wang J, Boomsma JJ, Zhang G**. 2014. Complementary symbiont contributions to plant decomposition in a fungus-farming termite. Proc Natl Acad Sci U S A **111**:14500–14505.

24. **Liu N, Zhang L, Zhou H, Zhang M, Yan X, Wang Q, Long Y, Xie L, Wang S, Huang Y, Zhou Z**. 2013. Metagenomic insights into metabolic capacities of the gut microbiota in a fungus-cultivating termite (*Odontotermes yunnanensis*). PLoS ONE **8**.

25. **Engel P, Martinson VG, Moran NA**. 2012. Functional diversity within the simple gut microbiota of the honey bee. Proc Natl Acad Sci U S A **109**:11002–11007.

26. **Koch H, Schmid-Hempel P**. 2011. Socially transmitted gut microbiota protect bumble bees against an intestinal parasite. Proc Natl Acad Sci U S A **108**:19288–19292.

27. **Kwong WK, Engel P, Koch H, Moran NA**. 2014. Genomics and host specialization of honey bee and bumble bee gut symbionts. Proc Natl Acad Sci U S A **111**:11509–11514.

28. **Martinson VG, Danforth BN, Minckley RL, Rueppell O, Tingek S, Moran NA**. 2011. A simple and distinctive microbiota associated with honey bees and bumble bees. Mol Ecol **20**:619–628.

29. **Koch H, Schmid-Hempel P**. 2012. Gut microbiota instead of host genotype drive the specificity in the interaction of a natural host-parasite system. Ecol Lett **15**:1095–1103.

30. **Campos MGR, Bogdanov S, de Almeida-Muradian LB, Szczesna T, Mancebo Y, Frigerio C, Ferreira F**. 2008. Pollen composition and standardisation of analytical methods. J Apic Res **47**:154–161.

31. **Quinlan RJ, Cherrett JM**. 1979. The role of fungus in the diet of the leaf-cutting ant *Atta cephalotes* (L.). Ecol Entomol **4**:151–160.

32. **Pinto-Tomás AA, Anderson MA, Suen G, Stevenson DM, Chu FST, Cleland WW, Weimer PJ, Currie CR**. 2009. Symbiotic nitrogen fixation in the fungus gardens of leaf-cutter ants. Science **326**:1120–1123.

33. **Andersen SB, Hansen LH, Sapountzis P, Sorensen SJ, Boomsma JJ**. 2013. Specificity and stability of the *Acromyrmex-Pseudonocardia* symbiosis. Mol Ecol **22**:4307–4321.

34. **Schloss PD, Westcott SL, Ryabin T, Hall JRA, Hartmann M, Hollister EB, Lesniewski R a, Oakley BB, Parks DH, Robinson CJ, Sahl JW, Stres B, Thallinger GG, Van Horn DJ, Weber CF**. 2009. Introducing mothur: open-source, platform-independent, community-supported software for describing and comparing microbial communities. Appl Env Microbiol **75**:7537–7541.

35. **Schloss PD, Gevers D, Westcott SL**. 2011. Reducing the effects of PCR amplification and sequencing artifacts on 16S rRNA-based studies. PloS One **6**:e27310.

36. **Quast C, Pruesse E, Yilmaz P, Gerken J, Schweer T, Yarza P, Peplies J, Glöckner FO**. 2013. The SILVA ribosomal RNA gene database project: improved data processing and web-based tools. Nucleic Acids Res **41**:D590–596.

37. **Huse SM, Welch DM, Morrison HG, Sogin ML**. 2010. Ironing out the wrinkles in the rare biosphere through improved OTU clustering. Environ Microbiol **12**:1889–1898.

38. **Kozich JJ, Westcott SL, Baxter NT, Highlander SK, Schloss PD**. 2013. Development of a dual-index sequencing strategy and curation pipeline for analyzing amplicon sequence data on the MiSeq Illumina sequencing platform. Appl Environ Microbiol **79**:5112–5120.

39. **Altschul SF, Gish W, Miller W, Myers EW, Lipman DJ**. 1990. Basic local alignment search tool. J Mol Biol **215**:403–410.

40. **Drummond AJ, Ashton B, Buxton S, Cheung M, Cooper A, Duran C, Field M, Heled J, Kearse M, Markowitz S, Moir R, Stones-Havas S, Sturrock S, Thierer T, Wilson A**. 2011. Geneious v5.4. Available httpwwwgeneiouscom.

41. **Therneau TM, Grambsch PM**. Modeling Survival Data: Extending the Cox Model.

42. **Therneau TM**. 2014. A Package for Survival Analysis in S. R package.

43. **Braig HR, Zhou W, Dobson SL, O'Neill SL**. 1998. Cloning and characterization of a gene encoding the major surface protein of the bacterial endosymbiont *Wolbachia pipientis*. J Bacteriol **180**:2373–2378.

44. **Andersen SB, Boye M, Nash DR, Boomsma JJ**. 2012. Dynamic *Wolbachia* prevalence in *Acromyrmex* leaf-cutting ants: potential for a nutritional symbiosis. J Evol Biol **25**:1340–1350.

45. **Lopez-Madrigal S, Balmand S, Latorre A, Heddi A, Moya A, Gil R**. 2013. How does *Tremblaya princeps* get essential proteins from its nested partner *Moranella endobia* in the mealybug *Planoccocus citri*? Plos One **8**.

46. **Poulsen M, Cafaro M, Boomsma JJ, Currie CR**. 2005. Specificity of the mutualistic association between actinomycete bacteria and two sympatric species of *Acromyrmex* leaf-cutting ants. Mol Ecol **14**:3597–3604.

47. **Seipke RF, Kaltenpoth M, Hutchings MI**. 2012. *Streptomyces* as symbionts: an emerging and widespread theme? FEMS Microbiol Rev **36**:862–876.

48. **Van Borm S, Wenseleers T, Billen J, Boomsma JJ**. 2003. Cloning and sequencing of *wsp* encoding gene fragments reveals a diversity of co-infecting *Wolbachia* strains in *Acromyrmex* leafcutter ants. Mol Phylogenet Evol **26**:102–109.

49. **Frost CL, Fernandez-Marin H, Smith JE, Hughes WO**. 2010. Multiple gains and losses of *Wolbachia* symbionts across a tribe of fungus-growing ants. Mol Ecol **19**:4077–85.

50. **Frost CL, Pollock SW, Smith JE, Hughes WOH**. 2014. *Wolbachia* in the flesh: symbiont intensities in germ-line and somatic tissues challenge the conventional view of *Wolbachia* transmission routes. PloS One **9**:e95122.

51. **Cox-Foster DL, Conlan S, Holmes EC, Palacios G, Evans JD, Moran NA, Quan P-L, Briese T, Hornig M, Geiser DM, Martinson V, vanEngelsdorp D, Kalkstein AL, Drysdale A, Hui J, Zhai J, Cui L, Hutchison SK, Simons JF, Egholm M, Pettis JS, Lipkin WI**. 2007. A metagenomic survey of microbes in honey bee colony collapse disorder. Science **318**:283–287.

52. **Fischer HM**. 1994. Genetic regulation of nitrogen fixation in Rhizobia. Microbiol Rev **58**:352–386.

53. **Kooij PW, Liberti J, Giampoudakis K, Schiøtt M, Boomsma JJ**. 2014. Differences in forage-acquisition and fungal enzyme activity contribute to niche segregation in Panamanian leaf-cutting ants. PloS One **9**:e94284.

54. **Sieber R, Leuthold RH**. 1981. Behavioural elements and their meaning in incipient laboratory colonies of the fungus-growing Termite *Macrotermes michaelseni* (Isoptera: Macrotermitinae). Insectes Sociaux **28**:371–382.

55. **Nobre T, Rouland-Lefèvre C, Aanen DK**. 2011. Comparative biology of fungus cultivation in termites and ants, p. 193–210. *In* Bignell, DE, Roisin, Y, Lo, N (eds.), Biology of Termites: a Modern Synthesis. Springer Netherlands.

56. **Otani S, Mikaelyan A, Nobre T, Hansen LH, Koné NA, Sørensen SJ, Aanen DK, Boomsma JJ, Brune A, Poulsen M**. 2014. Identifying the core microbial community in the gut of fungus-growing termites. Mol Ecol **23**:4631–4644.

57. **Poulsen M, Bot ANM, Currie CR, Boomsma JJ**. 2002. Mutualistic bacteria and a possible trade-off between alternative defence mechanisms in *Acromyrmex* leaf-cutting ants. Insectes Sociaux **49**:15–19.

58. **McGowin CL, Popov VL, Pyles RB**. 2009. Intracellular *Mycoplasma genitalium* infection of human vaginal and cervical epithelial cells elicits distinct patterns of inflammatory cytokine secretion and provides a possible survival niche against macrophage-mediated killing. BMC Microbiol **9**:139.

59. **Serbus LR, Casper-Lindley C, Landmann F, Sullivan W**. 2008. The genetics and cell biology of *Wolbachia*-host interactions. Annu Rev Genet **42**:683–707.

60. **Wright JD, Sjostrand FS, Portaro JK, Barr AR**. 1978. The ultrastructure of the rickettsia-like microorganism *Wolbachia pipientis* and associated virus-like bodies in the mosquito *Culex pipiens*. J Ultrastruct Res **63**:79–85.

61. **Kuykendall, LD**. 2005. p. 324-574. *In* Garrity, George, Brenner, Don J., Krieg, Noel R., Staley, James T. (eds.) Bergey's Manual® of Systematic Bacteriology: Volume Two: The Proteobacteria. Springer Science & Business Media.

62. **Fulcher TP, Dart JKG, McLaughlin-Borlace L, Howes R, Matheson M, Cree I**. 2001. Demonstration of biofilm in infectious crystalline keratopathy using ruthenium red and electron microscopy. Ophthalmology **108**:1088–1092.

63. **Kim JK, Kwon JY, Kim SK, Han SH, Won YJ, Lee JH, Kim C-H, Fukatsu T, Lee BL**. 2014. Purine biosynthesis, biofilm formation, and persistence of an insect-microbe gut symbiosis. Appl Environ Microbiol **80**:4374–4382.

64. **Heindl JE, Wang Y, Heckel BC, Mohari B, Feirer N, Fuqua C**. 2014. Mechanisms and regulation of surface interactions and biofilm formation in *Agrobacterium*. Plant-Microbe Interact **5**:176.

65. **Rasgon JL, Gamston CE, Ren X**. 2006. Survival of *Wolbachia pipientis* in cell-free medium. Appl Environ Microbiol **72**:6934–6937.

66. **Kautz S, Rubin BE, Russell JA, Moreau CS**. 2013. Surveying the microbiome of ants: comparing 454 pyrosequencing with traditional methods to uncover bacterial diversity. Appl Env Microbiol **79**:525–34.

67. **Larson HK, Goffredi SK, Parra EL, Vargas O, Pinto-Tomas AA, McGlynn TP**. 2014. Distribution and dietary regulation of an associated facultative Rhizobiales-related bacterium in the omnivorous giant tropical ant, *Paraponera clavata*. Naturwissenschaften **101**:397–406.

68. **Funaro CF, Kronauer DJC, Moreau CS, Goldman-Huertas B, Pierce NE, Russell JA**. 2011. Army ants harbor a host-specific clade of Entomoplasmatales bacteria. Appl Environ Microbiol **77**:346–350.

69. **Johansson H, Dhaygude K, Lindström S, Helanterä H, Sundström L, Trontti K**. 2013. A metatranscriptomic approach to the identification of microbiota associated with the ant *Formica exsecta*. PloS One **8**:e79777.

70. **Kautz S, Rubin BER, Moreau CS**. 2013. Bacterial Infections across the Ants: Frequency and Prevalence of *Wolbachia, Spiroplasma*, and *Asaia*. Psyche J Entomol **2013**:e936341.

71. **Taylor-Robinson D, Bébéar C**. 1997. Antibiotic susceptibilities of mycoplasmas and treatment of mycoplasmal infections. J Antimicrob Chemother **40**:622–630.

72. **De Souza DJ, Bezier A, Depoix D, Drezen JM, Lenoir A**. 2009. *Blochmannia* endosymbionts improve colony growth and immune defence in the ant *Camponotus fellah*. BMC Microbiol **9**:29.

73. **Keller L, Liautard C, Reuter M, Brown WD, Sundström L, Chapuisat M**. 2001. Sex ratio and *Wolbachia* infection in the ant *Formica exsecta*. Heredity **87**:227–233.

74. **Wenseleers T, Sundström L, Billen J**. 2002. Deleterious *Wolbachia* in the ant *Formica truncorum*. Proc R Soc B Biol Sci **269**:623–629.

Acknowledgements

Funding was provided by a Danish National Research Foundation grant (DNRF57) and an ERC Advanced Grant (323085) to JJB, and an Intra-European Marie Curie Fellowship to PS hosted by MS and JJB (300584 GUTS FP7-PEOPLE-2011-IEF). We thank the University of Michigan Host Microbiome Initiative (HMI) for the library preparation and advice about Miseq sequencing, the Mothur forum for help with the analysis, Severine Balmand for providing the protocol for the FISH microscopy, Mette Boye and Anders Garm for access to the confocal microscope facilities, Sylvia Mathiasen, Karin Vestberg, Saria Otani and Pepijn Kooij for lab assistance, Jelle van Zweden and David Nash for help with the statistics, Dani Moore for rearing one of the colonies, and Michael Poulsen for comments on an earlier version of the manuscript. TEM imaging data were collected at the Center for Advanced Bioimaging (CAB) Denmark, University of Copenhagen, and at the facilities of the Interinstitutional Shared Centre for Microscopic Analysis of Biological Objects, Institute of Cytology and Genetics, Siberian Branch of the Russian Academy of Sciences. The Smithsonian Tropical Research Institute in Panama made lab facilities available during fieldwork, and the Autoridad Nacional del Ambiente of Panama issued collection and export permits.

Figure Legends

Figure 1: Combined 16S sequencing results for the gut microbiomes of sympatric colonies of *A. echinatior*, *A. octospinosus* and *A. volcanus* using both Roche 454 and Illumina Miseq 16S-sequencing. OTU Heatmaps showing the relative abundances (rarefied number of reads) of the four most abundant OTUs identified initially with 454 sequencing (details in text and Table S4) in lab samples (>2 years after collection) consisting of five pooled large worker guts per colony and afterwards confirmed by Miseq sequencing of field colony samples (F) and repeated samples of

747 these colonies 3 months after transfer to the lab (3m). From left to right: relative abundances of the
748 11 lab colony samples, sequenced with 454 (white, shades of gray to red heatmap) and the 19
749 samples sequenced with Illumina Miseq (white, shades of gray to green heatmap), consisting of six
750 F plus 3m colonies, six long-term lab colonies that had already been sequenced with 454, and a new
751 long-term lab colony sample (Ao273). We compared OTU nucleotide sequences from both runs
752 using blastn with a 100% identity and 1e-50 evalue cutoff, after which we checked whether OTUs
753 from different platforms had identical nucleotide sequences (100%), the same classification and the
754 same distribution across samples (colonies) before concluding that they represented the same OTU.
755 Top dendrograms above the heatmaps segregate the microbiomes based on weighted Euclidean
756 distances of community similarity. Pie charts at the bottom give cumulative abundances of these
757 four OTUs (black) versus the 176 other OTUs (white) that were identified in the 454 run and the
758 198 other OTUs (white) that were identified in the Miseq run. The arrows and the numbers at the
759 bottom highlight the six identical samples that were sequenced in both runs.
760
761 **Figure 2: Distribution and structural organization of dominant bacteria in gut tissues of**
762 ***Acromyrmex* leaf-cutting ants.** Schematic diagram of gut tissues sampled **(A)**. FISH of
763 Entomoplasmatales (green, EntomA_Cy3 probe) and Rhizobiales (red, Phyllo_Cy5 probe) in a fat
764 body cell (**B**) and a Malpighian tubule (**C**), showing that Entomoplasmatales (Mollicutes) are
765 always present but Rhizobiales absent. *Wolbachia* (green; Wolb_Cy3 probe, W2_Cy3 probes and
766 red, wsp_Cy5 probe) in a fat body cell (**D**). Entomoplasmatales (Mollicutes) (green, Entom_A488
767 probe) in optical sections of parts of the ileum (**E**) and rectum (**F**) where α-proteobacteria are absent
768 (Phyllo_Uni_Cy5 probe). *Wolbachia* (green; Wolb_Cy3 probe) and Rhizobiales (red; Phyllo_Cy5
769 probe) in other sections of the ileum (**G**) and rectum (**H**). White arrows indicate Entomoplasmatales
770 (Mollicutes; **B-F**), yellow arrows *Wolbachia* (**D**,**G**), and arrowheads Rhizobiales (**G,H**); frames in

matching colors (**G,H**) show bacteria at higher magnification. DNA was stained with DAPI (blue). Mollicutes were present in almost all tissues examined (**A-F**), Rhizobiales only in the ileum (**G**) across the cuticle (marked with c), the epithelium (marked with e) and in the rectum (**H**), while *Wolbachia* was only sporadically observed in the lumen but abundantly in the fat body cells (**D,G**). Electron microscopy images of an Entomoplasmatales bacterium in a fat body cell, with the inset showing that the bacterial cell wall is lacking and black arrows indicating that cells are surrounded by a plasma membrane and a membrane of host origin (**I**). Dividing Entomoplasmatales in the lumen of the rectum, with the inset showing the single plasma membrane that is characteristic for free-living Entomoplasmatales (**J**). A rod-shaped Rhizobiales bacterium in the ileum (**K**). A *Wolbachia* bacterium in a fat body cell, with inset and black arrowheads showing its typical endosymbiotic three-layered envelope (**L**). Scale bars are 10 µm (**B-H**) and 0.5 µm (**I-L**). Critical interpretational images presented in this figure were also obtained for *A. octospinosus* and did not reveal any significant differences with *A. echinatior*.

Figure 3: Presence of Rhizobiales bacteria and bacterial *nifH* genes and NifH proteins in the hindgut of *Acromyrmex octospinosus* leaf-cutting ant workers. *NifH*-specific PCR of DNA extracted from *A. octospinosus* guts showing weak positive signals in fat body and Malpighian tubule cells and a strong signal in the rectum/ileum, whereas only the strong rectum/ileum signal could be retrieved from ants that were kept on sucrose diet for 15 days. All signals were confirmed to be *nifH* by Sanger sequencing and shown to be either identical or most closely related to known *nifH* sequences of Rhizobiales (10/12 sequences) or to give similarly close matches to both Rhizobiales and non-Rhizobiales bacteria (2/12 sequences: 18cl8_Ae342 and QC8_Ae342) (see text for details) (**A).** Immunofluorescence image confirming the NifH protein (bright red dots) close to the cuticle of the ileum and covering or being directly adjacent to the bacterial DNA signals (blue

795 dots: stained by DAPI). The host DNA of the epithelium (e) was also visible. The inset frames show
796 magnifications of red stained dots representing NifH and DAPI signals (**B**). Electron microscopy
797 image showing Rhizobiales bacteria close to the rectal cuticle and surrounded by a low-density
798 matrix (**C**), at a higher magnification (**D**), and similar in the ileum (**E**). Polysaccharides detected by
799 PAS staining in the ileum of ants kept for two weeks on a sterile sucrose diet without fungus
800 garden, showing the Rhizobiales biofilm at low (**F**) and high magnification (**G;** rectangle frame in
801 **F**). Scale bars are 10µm (**B**), 1µm (**C**-**E**), 50µm (**F**) and 10µm (**G**).

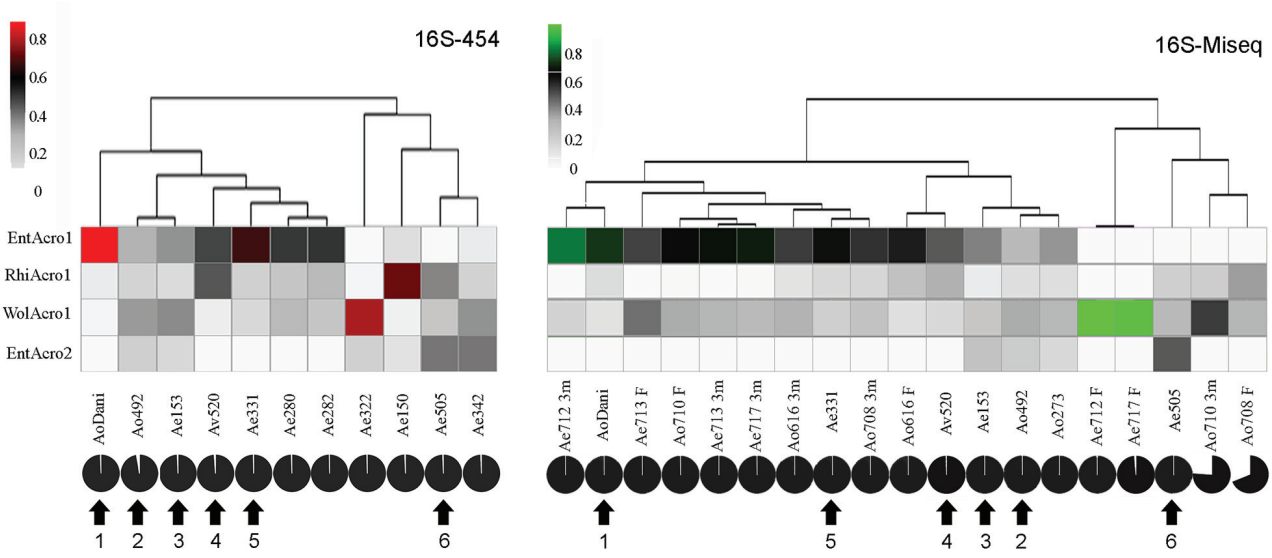

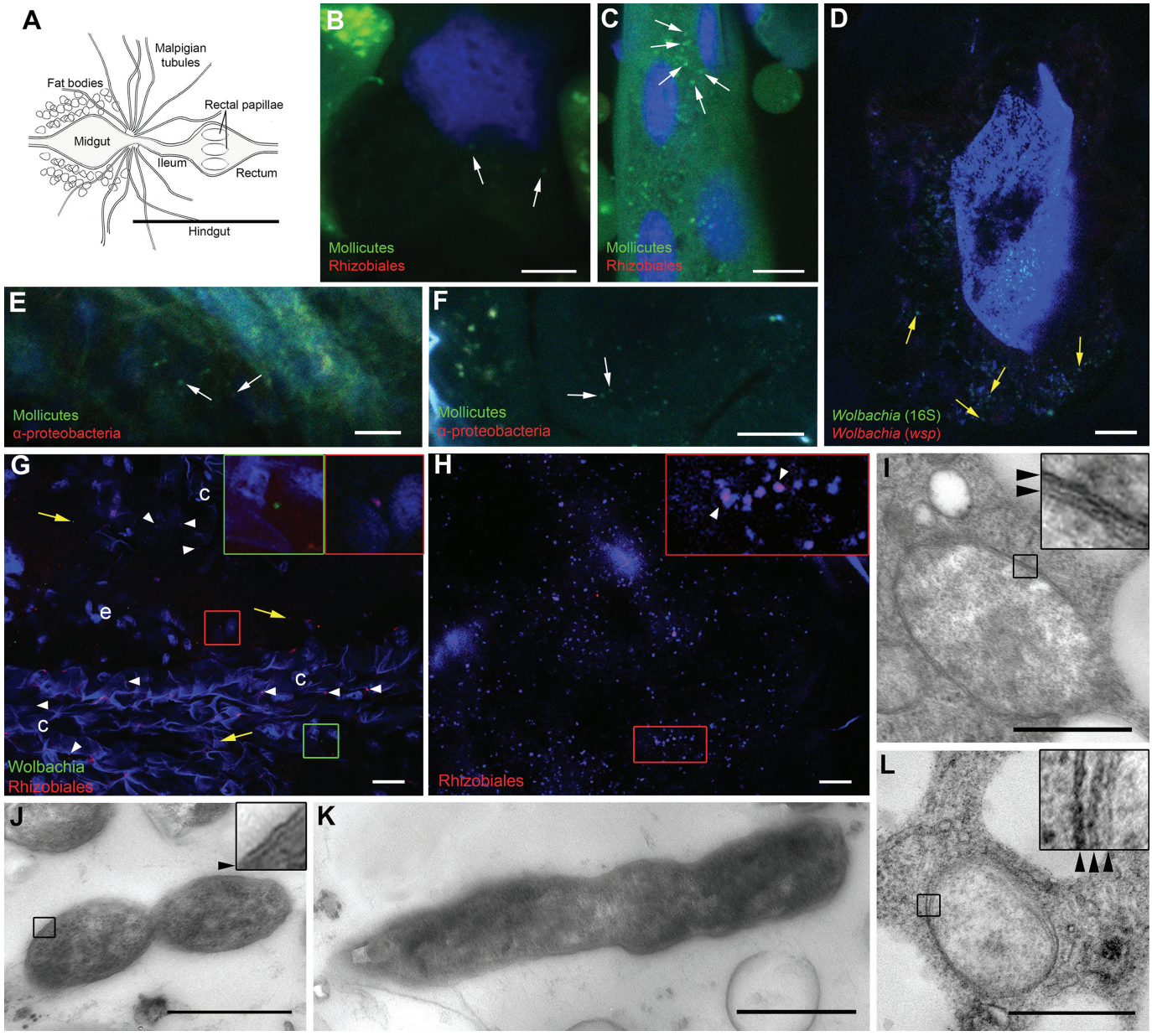

Applied and Environmental Microbiology

AEM

Applied and Environmental Microbiology